MAGNETIC CHICANE RADIATION STUDIES AT THE BNL ATF*

M. Dunning, G. Andonian, A.M. Cook, E. Hemsing, A. Murokh, S. Reiche, J. Rosenzweig,
D. Schiller, Particle Beam Physics Laboratory, Department of Physics and Astronomy, UCLA,
Los Angeles, CA 90095, USA
M. Babzien, K. Kusche, V. Yakimenko, Accelerator Test Facility, Brookhaven National Laboratory
Upton, NY 11973, USA.

Abstract

Radiation emitted by relativistic electrons traversing the magnetic eld gradients of a chicane bunch compressor has been studied in an attempt to characterize coherent edge radiation (CER). The studies performed at the Accelerator Test Facility (ATF) at Brookhaven National Laboratory (BNL) include frequency spectrum, angular distribution, and polarization measurements. A reconstruction of the longitudinal charge pro le from the measured spectrum shows that the bunch has been compressed to approximately 30 μm FWHM, with a peak current exceeding 1.5 kA. Measurements of radiation from the short pulses are compared to predictions from `QUINDI`, a new simulation code developed at UCLA to model the radiation.

INTRODUCTION

The chicane compressor studies are a collaboration with the Particle Beam Physics Laboratory (PBPL) at UCLA and the ATF, the user facility which hosts the experiment. The chicane was designed to compress the electron beam to yield the high peak current necessary to drive a self-ampli ed spontaneous emission free electron laser (SASE FEL) to saturation [1] and to expand the ATF core capabilities. Recent experiments have focused on the creation of very short electron beam pulses ($\sim$30 μm), and measurements of CER and coherent synchrotron radiation (CSR) emitted by such short bunches. The correlation between these radiative effects and microbunching instabilities are under investigation, as are other parasitic effects of the radiation. These are signi cant issues for larger projects, such as the Linac Coherent Light Source (LCLS), which will employ similar devices and diagnostics for the production of short duration pulses. CER has also been shown to be a bright source of infrared radiation, which makes it well-suited for certain types of microscopy and spectroscopy [2].

* Work supported by DOE grant DE-FG02-98ER45693 and NSF grant PHY-0355048.

EXPERIMENT DESCRIPTION

Chicane Compressor

The chicane compressor is currently installed along the high-energy line (H-line) of the ATF. The operating beam energy is 60-61 MeV for the present chicane radiation studies. The compressor consists of four dipole magnets oriented in a chicane layout, as in Fig. 1.

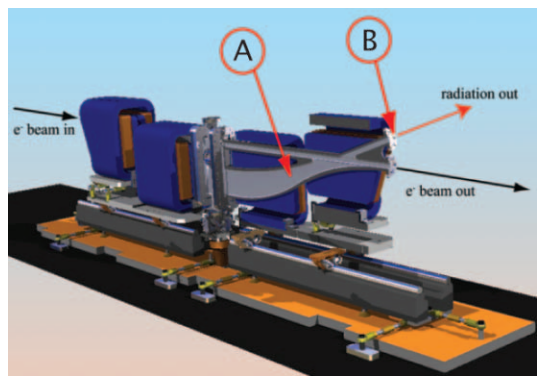

Figure 1: A rendering of the four dipole chicane compressor. The cutaway view shows the approximate radiation source between the third and fourth dipoles (A) and the radiation extraction port (B).

The chicane features a dedicated radiation extraction port that enables viewing of the region (Fig. 1A) which extends through the downstream edge of the third magnet to the upstream edge of the fourth magnet. The rectangular exit port (Fig. 1B) has transverse dimensions of 26 mm $\times$ 11 mm, with the longer dimension in the bend plane [3].

Table 1: Chicane design parameters

Parameter	Value	Units
B-Field	2015	Gauss
Bend Angle	20	deg
Geometric Length	41	cm
Magnet Gap	2.1	cm

Terahertz Radiation Transport

Radiation exits the chicane compressor through a fused silica vacuum window located on the extraction port (Fig. 1B). The radiation is guided with three adjustable mirrors (gold-coated) and a translatable Picarin lens, through metallic pipes (56 mm diameter) to an external diagnostic station. The entire length of the radiation transport line is approximately 7 m. The Picarin lens is positioned one focal length (1.25 m) from the approximate radiation source (between the third and fourth dipoles) to achieve a point-to-parallel transport con guration.

Diagnostic Station

The diagnostic station located at the end of the radiation transport is designed to be modular for versatility. It consists of focusing/turning mirrors, two individual l-ter wheels containing room temperature and cryogenically cooled lters, a wire grid polarizer, an iris on a two-dimensional translation stage, a silicon bolometer, and a Michelson-type interferometer.

Silicon Bolometer

In order to characterize the chicane radiation, a cryogenically cooled silicon bolometer (IR Labs model HDL-5) is employed. The bolometer is cooled with liquid helium and has a built in lter wheel, loaded with cut-on lters (long-pass) with wavelengths of 13, 27, 45, 103, and 285 μm. The detector element incorporates a Winston Cone collector, protected by a wedged polyethylene window (that provides an additional cut-on wavelength of 13 μm) [4].

Interferometer

The radiation spectrum is measured at the output of a Michelson-type interferometer as a function of bolometer voltage. The interferometer is optimized for the 15 μm to 1 mm wavelength range, and has a translatable mirror along one orthogonal leg with 1 μm spatial resolution [5].

CHICANE RADIATION OVERVIEW

Radiation exiting the chicane contains features of both synchrotron and edge radiation due to the measurement position and the magnet geometry. For electrons emitting under the same radiation process, the far- eld intensity distribution is expressed as

$$\mathscr{I}(\omega) = \mathscr{I}_0(\omega)[N_e + N_e(N_e - 1)F(\omega)], \qquad (1)$$

where $\mathscr{I}_0(\omega)$ is the single electron intensity distribution and $F(\omega)$ is the bunch form factor. For wavelengths longer than the bunch length ($\sim$ 30 μm), each type of radiation is coherently enhanced by a factor of N_e, the number of electrons in a bunch. Typically, $N_e \sim 10^9$ for the present ATF running parameters.

The edge radiation emitted from electrons entering and exiting the edges of bend magnets is expected to have greater intensity at longer wavelengths than synchrotron radiation [6]. The characteristics of CER also depend on the topology of the eld gradient. In the *zero-edge length model* [7], the eld of the bending magnet is approximated by a step function. The resultant radiation is radially polarized, with a cylindrically symmetric spatial distribution characterized by a null on the straight section axis and maxima at $\theta \sim 1/\gamma$, analogous to transition radiation. Analytic nite edge length models result in complicated expressions, requiring numerical calculations [8].

Simulations

Start-to-end simulations for the experiment were conducted with `PARMELA` [9] for the electron beam dynamics in the accelerating modules. The code `QUINDI` was used for the beam transport and radiation studies.

`QUINDI` is a parallel-computing code speci cally developed to model the emitted radiation from electron bunches within the ATF chicane. The program avoids the sequential approach of a magnetic lattice, relying instead on an object-driven description of magnetic elements. The observed radiation eld is calculated on a user-de ned plane based on the acceleration eld of the Liénard-Wiechert potentials.

MEASUREMENTS AND ANALYSIS

Frequency Spectrum

Spectral measurements of the emitted chicane radiation were conducted at the ATF. Interferograms were obtained from scans with the Michelson-type interferometer to provide information about the spectral content. This data was used to reconstruct the longitudinal charge distribution of the beam.

Interferometer signal amplitudes from the output of the silicon bolometer were recorded for N shots per mirror position. An averaged, normalized interferogram with the corresponding measured electron beam charge is shown in Fig. 2(a). Each point on the interferogram records the mean value and the error bars depict the standard deviation.

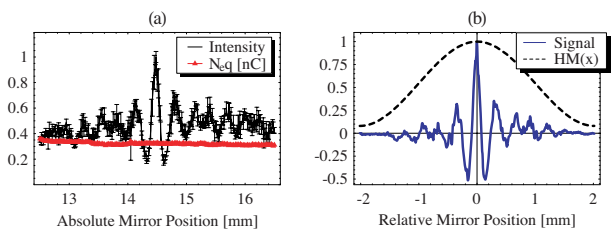

Figure 2: (a) Normalized, averaged signal amplitudes from interferometer scans of chicane radiation. (b) Apodized signal via a Hamming function.

For an accurate spectral reconstruction with a Discrete Inverse Fourier Transform (DIFT), the non-zero offset of the interferogram is removed and the signal is multiplied by an apodization function. Fig. 2(b)

shows the results of apodization by a Hamming function $\mathrm{HM}(x) = 0.54 + 0.46\cos(\frac{\pi x}{a})$, where $2a = 4$ mm is the length of the interferometer scan centered on the maximum peak. This standard procedure removes arti cial low-frequency components and corrects for the spurious tails that arise from the nite sum in the DIFT [10],

$$\tilde{I}_k = \frac{1}{n}\mathrm{Re}\sum_{j=1}^{n} I_j e^{2\pi i(k-1)(j-1)/n}, \qquad (2)$$

where n is the number of equally spaced interferometer mirror positions recorded over a nite distance $[ct_{min}, ct_{max}]$. This yields $n/2$ non-repeating intensity values, I_k, up to the maximum frequency, where I_j is the j^{th} intensity point in the modi ed interferogram.

Fig. 3(a) displays the resulting spectrum of the apodized signal. The peak at $f_{peak} \approx 0.5$ THz coincides with the dominant frequency given by results from QUINDI simulations.

Kramers-Kronig Reconstruction

The forward far- eld radiation intensity spectrum produced by the bunch is given by Eq. 1, where the longitudinal form factor $F(\omega)$ is

$$F(\omega) = \left| \int \hat{\rho}(z) e^{i\omega z/c} dz \right|^2, \qquad (3)$$

with $\hat{\rho}(z) = \rho(z)/N_e q$, the normalized longitudinal charge density. Following a minimal-phase reconstruction technique, a discretized Kramers-Kronig relation is used to extract $\hat{\rho}(z)$ [11].

The minimal phase is

$$\psi(\omega_i) = \frac{2\omega_i}{\pi}\sum_{j\neq i}^{N_{max}} \frac{\ln[\xi(\omega_j)/\xi(\omega_i)]}{\omega_j^2 - \omega_i^2}\Delta\omega, \qquad (4)$$

where $\xi^2(\omega_i) = F(\omega_i)$, and $\Delta\omega$ is the resolution from the spectrum. The normalized pro le $\hat{\rho}(z)$ then has the form

$$\hat{\rho}(z) = \frac{1}{\pi c}\sum_{i=0}^{N_{max}} \xi(\omega_i)\cos\left[\psi(\omega_i) - \frac{\omega_i z}{c}\right]\Delta\omega. \qquad (5)$$

The bunch distribution is calculated from the form factor, determined by tting well-behaved asymptotes to the measured normalized spectrum. Results of this reconstruction are shown in Fig. 3(b). The values for current are scaled to the average measured charge of $N_e q \approx 330$ pC. Due to experimental limitations (discussed below) and numerical tting of the form factor, this reconstruction technique is useful as an approximation of the true bunch distribution. Nevertheless, the reconstructed pro le shows general agreement with predictions from PARMELA simulations in the overall structure of the asymmetric bunch and the compressed head of ~ 30 μm FWHM.

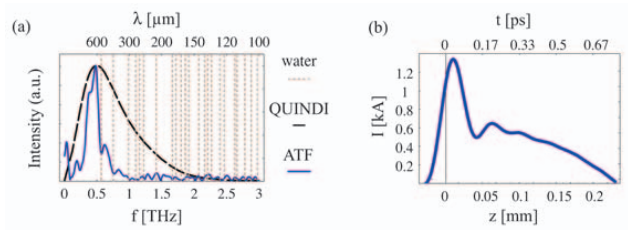

Figure 3: (a) Spectra from apodized interferogram and from simulation. Prominent water absorption frequencies are shown as vertical dotted lines. (b) Minimal phase Kramers-Kronig bunch reconstruction for the measured spectrum.

Limitations on Spectral Analysis

The simulated and measured spectra show that the radiation is dominated by frequencies below 1.5 THz, however, several experimental factors contribute to spectral l-tering which affect the measured frequency distribution and the longitudinal bunch reconstruction. The primary experimental artifact near the dominant frequency band is the selective ltering from water absorption (due to high levels of humidity encountered through the radiation transport on the dates of data acquisition). This effect is exempli ed by strong absorption troughs located near $f = 0.57$ and 0.75 THz. Signi cant absorption frequencies are plotted in Fig. 3(a) for a 7 m travel path [12]. The spectrum is also affected by the radiation transport line, which acts as a high pass lter due to its inherent nite apertures and acceptance angles. Further, the fused silica vacuum port window maintains a transmission coef cient that slowly decreases for frequencies greater than 0.3 THz, but rapidly approaches zero for frequencies greater than 6 THz.

Polarization

The transverse radiation pro le and polarization were measured in an effort to observe the distinctions between CER and CSR. Fig. 4 shows the measured intensity (normalized to maximum) as a function of polarizer rotation angle. The wire grid polarizer was mounted at the end of the transport and rotated in 15° increments, and the focused signal intensity was measured with the bolometer. The linearly polarized component of radiation (sinusoidal) is consistent with that expected from synchrotron radiation. The non-linearly polarized component, which introduces a vertical offset, is a clear signature of edge radiation. Analytic studies show that pure synchrotron radiation would give a ratio of approximately 7:1 between the maximum and minimum signal [13], while the observed ratio is approximately 4:1. QUINDI results are consistent with the measured data (Fig. 4).

Transverse Spatial Distribution

The transverse far- eld spatial intensity distribution of the emitted radiation was measured by scanning a small iris

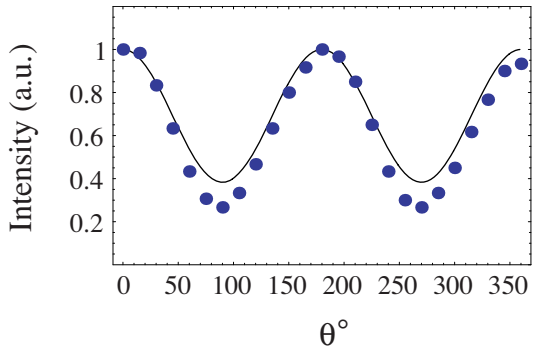

Figure 4: Normalized polarization intensity of the chicane radiation. Solid line is from QUINDI, dots are measured at the bolometer. The zero angle is arbitrary.

(3 mm diameter) in a 19 mm × 23 mm rectangular array of discrete points (Δd =3.8 mm). The iris was scanned across the transport tube exit and the signal was focused into the bolometer. Iris scans were performed for varying radiation polarizations with the aforementioned wire-grid polarizer (Fig. 5).

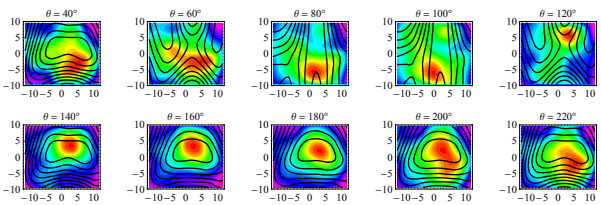

Figure 5: Interpolated far- eld radiation intensity distributions for 20 degree polarizer angle increments, with results from QUINDI simulations (contours) overlayed for comparison. The x and y scales have units of mm.

CONCLUSION

The chicane radiation studies at the ATF display telling signatures of edge radiation. The transverse spatial distributions show patterns consistent with simulations, namely strong peaks shifting into multiple peaks for varying degrees of polarization with identi able nulls in the distribution on-axis. The non linearly polarized component of radiation observed as an offset to the sinusoidal signal in the overall polarization curve is a clear indication of the actuality of prominent edge radiation.

Future plans to improve the measurements include radiation transport modi cations such as replacement of the fused silica chicane radiation port window with a diamond or z-cut crystalline quartz window; this will greatly improve the spectral range of the measurements. In addition, enclosing and ushing the transport line with dry nitrogen will mitigate the effects of water absorption lines in the measured spectrum. Also, a Czerny-Turner type monochromator is currently being built in order to more ef ciently resolve the chicane radiation spectrum.

REFERENCES

[1] G. Andonian, *et al.*, *Proceedings of the 2003 Particle Accelerator Conference*, 944, 2003.

[2] T. E. May, R. A. Bosch, and R. L. Julian, *Proceedings of the 1999 Particle Accelerator Conference*, 2394, 1999.

[3] R. Agustsson, *UCLA M.S. Thesis* (2003).

[4] http://www.irlabs.com/.

[5] http://www.radiabeam.com/.

[6] O. V. Chubar and N. V. Smolyakov, *J. Optics (Paris)* **24**, 117 (1993).

[7] R. A. Bosch, *Il Nuovo Cimento* **20D**, 483 (1998).

[8] O. V. Chubar and N. V. Smolyakov, *Proceedings of the 1993 Particle Accelerator Conference*, 1626, 1993.

[9] E. Colby, *UCLA PhD Thesis*, FERMILAB-THESIS-1997-03 (FNAL, 1997).

[10] J. F. Rabolt and R. Bellar, *Applied Spectroscopy* **35**, 132, 1981.

[11] R. Lai and A.J. Sievers, *Phys. Rev. E* **50**, 5 (1994).

[12] P.U. Jepsen, *private communication*.

[13] J.D. Jackson, *Classical Electrodynamics*, John Wiley and Sons, New York, 1999.